CONTROL OF THE MAYA AUV IN THE VERTICAL AND HORIZONTAL PLANES: THEORY AND PRACTICAL RESULTS

Pramod Maurya, E. Desa, A. Pascoal[†], E. Barros[††], G. Navelkar, R Madhan, A. Mascarenhas , S. Prabhudesai, S.Afzulpurkar, A. Gouveia, S. Naroji, L. Sebastiao[†]

National Institute of Oceanography
Goa, India
maurya@nio.org
[†] *IST/ISR ,Lisbon, Portugal (antonio@isr.ist.utl.pt)*
[††] *University of SãoPaulo, SP, Brazil (eabarros@usp.br)*

Abstract: The paper describes the design and testing of the depth and heading autopilots for a small Autonomous Underwater Vehicle (AUV) named Maya. Control system design is done using the LQ (Linear-Quadratic) optimization technique based on a mathematical model of the AUV obtained by resorting to analytical and semi-empirical methods. Details of system implementation are given and the results of tests with the prototype vehicle are discussed. The paper concludes with a discussion of the interaction between motions in the horizontal and vertical planes due to an asymmetry in the placement of the stern control planes.

Keywords: Autonomous underwater vehicle, Depth Control, Heading Control.

1. INTRODUCTION

Our first thoughts on the development of a small AUV for Oceanography began in 1998 with the suggestion that ship time at a cruise station could be exploited by having small autonomous underwater vehicles, suitably equipped with oceanographic sensors, to sample the ocean in the vertical and horizontal dimensions of the space around the ship. In other words, we were thinking of an 'extended arm of an oceanographic research vessel', so the evolution of Maya took place. Maya is a small AUV developed at the National Institute of Oceanography (NIO), Goa, India.

Fig 1. Small AUV developed at NIO, Goa

Fig 2. Maya cruising underwater

Part of the research and development effort that led to MAYA was carried out in the scope of an on-going Indian-Portuguese collaboration programme that aims to build and test the joint operation of two AUVs for marine science applications. This collaborative research was also extended to the Univ. São Paulo, Brazil to take advantage of their expertise on AUV modeling and parameter estimation.

2. VEHICLE MODEL

The MAYA AUV has a streamlined torpedo-like body propelled by a single thruster. For vehicle maneuvering, two stern planes and a single stern rudder underneath the hull are used. For simplicity, we assume that the complete six degrees of freedom model for the AUV can be split into two noninteracting models for the vertical and horizontal planes, see (Bjorn Jalving, 1994). The linearized dynamic equations of motion for the vertical and horizontal planes are represented in matrix form as

$$\begin{bmatrix} m-Z_{\dot{w}} & -Z_{\dot{q}} & 0 & 0 \\ -M_{\dot{w}} & I_{yy}-M_{\dot{q}} & 0 & 0 \\ 0 & 0 & 1 & 0 \\ 0 & 0 & 0 & 1 \end{bmatrix} \begin{bmatrix} \dot{w} \\ \dot{q} \\ \dot{\theta} \\ \dot{z} \end{bmatrix} + \begin{bmatrix} -Z_w & mu_0-Z_q & 0 & 0 \\ -M_w & -M_q & \overline{BG}_z W & 0 \\ 0 & -1 & 0 & 0 \\ -1 & 0 & u_0 & 0 \end{bmatrix} \begin{bmatrix} w \\ q \\ \theta \\ z \end{bmatrix} = \begin{bmatrix} Z_\delta \\ M_\delta \\ 0 \\ 0 \end{bmatrix} \delta_s \quad (1)$$

and

$$\begin{bmatrix} m-Y_{\dot{v}} & -Y_{\dot{r}} & 0 \\ -N_{\dot{v}} & I_{zz}-N_{\dot{r}} & 0 \\ 0 & 0 & 1 \end{bmatrix} \begin{bmatrix} \dot{v} \\ \dot{r} \\ \dot{\psi} \end{bmatrix} + \begin{bmatrix} -Y_v & -Y_r+mu_0 & 0 \\ -N_v & -N_r & 0 \\ 0 & -1 & 0 \end{bmatrix} \begin{bmatrix} v \\ r \\ \psi \end{bmatrix} = \begin{bmatrix} Y_\delta \\ N_\delta \\ 0 \end{bmatrix} \delta_r \quad (2)$$

respectively. The notation used in this paper is in accordance with (SNAME, 1950). The generalized velocity vector $\upsilon = [u\ v\ w\ p\ q\ r]'$ consists of surge, sway, heave, roll rate, pitch rate, and yaw rate and is expressed in body coordinates. The vector of Euler angles $\eta = [\varphi\ \theta\ \psi]'$ consist of roll, pitch, and yaw angles. Following the partition above, the state variables adopted are $[w, q, \theta\ z]'$ for the vertical plane and $[v, r, \psi]'$ for the horizontal plane. The control vector $u = [\delta r\ \delta s]'$ consists of rudder deflection δr and stern plane deflection δs. $\overline{BG}z$ is the separation between the centre of mass and the centre of buoyancy, W is the weight of the vehicle, and u_0 is the steady state speed of the surge speed of the vehicle about which the above linearized models are computed. The vehicle parameters were estimated by resorting to analytic and semi-empirical methods, see (Barros *et. al.*, 2004). The models were then linearized about the nominal cruising speed of 1.2 m/s. Details of the vehicle model for Maya are given below.

Physical Parameters
Nominal Vehicle Speed (u_0): 1.2 m/s
Reynolds Number: 1.6692e+006,
Sea Water Density: $\rho = 1025$ kg/m^3

Vehicle Parameters
Length (Lpp): 1.8 m,
Centre of mass (Zg): 0.52e-2 m (w.r.t body axis)
Centre of Buoyancy (Zb): -0.172e-2 m (w.r.t body axis)
Weight (W) = 53 x 9.8 Kgf
Buoyancy (B) = 53.4 x 9.8 Kgf
The dimensionless values of hydrodynamic coefficients for the vehicle are shown in table 1

Parameter	Value
Vertical Plane	
Z'_w	- 1.027e-1
Z'_δ	- 4.03e-2
M'_w	- 8.33e-3
M'_δ	- 7.87e-3
Z'_q	- 1.96e-2
M'_q	- 6.42e-3

Table 1. Foil–body–duct combination: hydrodynamic coefficients

The dimensionless values of added masses (see Barros *et. al.*, 2004) and moments of inertia for the vehicle are shown in table 2.

Parameter	Value
Vertical Plane	
$Z'_{\dot{w}}$	-2.98e-2
$Z'_{\dot{q}}$	8.22e-4
$M'_{\dot{w}}$	8.22e-4
$M'_{\dot{q}}$	-1.91e-3
I_{yy}	1.02e-3

Table 2. Added masses and moments of inertia

The derivatives for the horizontal plane are similar. The difference in signs and the effect of only one rudder used for horizontal plane has been taken into consideration.

The vehicle speed for the vehicle is set externally by the propeller revolutions and is not controlled explicitly. The only inputs considered are therefore common mode stern plane deflection and stern rudder deflection for the vertical and horizontal planes, respectively. However, the simplifying assumption that the vehicle motions in both planes are essentially non-interacting is not strictly valid. A depth-heading interaction was observed in field tests and this is discussed in Section 5.

3. CONTROL IN THE VERTICAL PLANE

In our control system design only three states $[q, \theta, z]'$ were accessible for measurement. The heave equation was neglected. This procedure is often adopted in practice to simplify the controller design, see (Bjorn Jalving, 1994). In our case, this strategy proved adequate because the vehicle is stern dominant and simulation results with the full model showed that the model simplification did not impact negatively on closed-loop maneuvering performance. Of course, this procedure cannot be accepted universally and may fail completely when the vehicle is bow dominant (open-loop "unstable")

while the artificial, reduced order mode is stable. This is not the case with the MAYA AUV.

3.1 Design and Simulation

Control system design was done by resorting to the LQ (linear, quadratic) design methodology (Lurie *et. al, 2000*). This was done by including the depth state z, together with its integral ∫z in the state variables to be penalized. This technique has the purpose of ensuring zero steady state error in response to step commands in depth. At the same time, it allows for simple implementation of the final controller using the Delta-implementation strategy described in (Kaminer *et. al, 1995)*. Thus, in the final state space model the state vector is [q, θ, z, ∫z]´. To apply the LQ design methodology, the extended vertical plane model was written in state-space form as

$$\dot{x}(t) = Ax(t) + Bu(t) \quad (3)$$

where matrices A and B can be derived from eq. (1), and x(t) and u(t) represents state and control vector, respectively. The cost criterion to be minimized, adopted in the LQR design, was

$$J = \int_0^\infty (x^T(t)Qx(t) + u^T(t)Ru(t))\,dt \quad (4)$$

where *Q* and *R* are weighting matrices. Under generic stabilizability and detectability assumptions, the solution to the above minimization problem yields a stabilizing state-feedback control law

$$u(t) = -K(t) \cdot x(t) \quad (5)$$

where K is a matrix of feedback gains. The Control System Tool box of Matlab™ was used to compute the optimal gain matrix K.

Weighting matrix: $Q = C^TC$

$C = [W_q \quad W_\theta \quad W_z \quad W_{\int z}]$

$= [\ 1 \quad 1 \quad 0.01 \quad 0.1]$

R = 0.5

After several iterations aimed at meeting time and frequency-domain requirements, the gains were found to be

K = [-0.90353 -1.3544 0.3817 0.044721]

The corresponding bandwidth of the closed loop system is 0.214 rad/sec, well within the natural bandwidth of the actuators. The closed loop eigen values are

Eigenvalue	Damping	Freq. (rad/s)
-0.264	1.00e+000	2.64e-001
-0.289 + 0.257i	7.47e-001	3.87e-001
-0.289 – 0.257i	7.47e-001	3.87e-001
-1.12	1.00e+000	1.12e+000

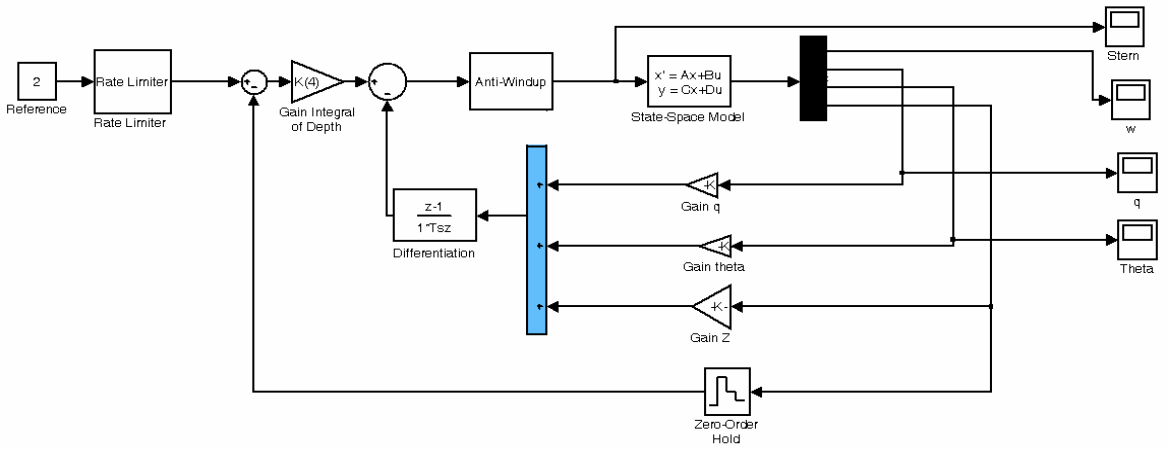

Figure 3 Simulation of Depth Control

The LQR structure was modified to accept reference commands in depth (figure 3). The final structure adopted was obtained by following the methodology described in (Kaminer *et. al,* 1995). The control law with the delta implementation is

$$\delta = \int \left[K_4(z_d - z) - \frac{d}{dt}(K_1 q + K_2\theta + K_3 z) \right] dt \quad (6)$$

where z_d is the desired depth, z is the measured depth, θ is the pitch angle, and q is the pitch rate.

The performance of the depth control system was assessed in simulation and the results are shown in figures 4 and 5. In the simulation, the controller was discretized at a sampling time of 0.1 seconds. A pre-filter on depth commands was used as a depth rate limiter to limit high pitch angles during descent and ascent of the vehicle. Anti-windup was used to switch off the integral action during saturation of the actuator which is set to ± 20˚. In simulation, the vehicle was commanded to dive to the depths of 1.5 and 2 meters and to return to 1.5 meters. The

corresponding pitch angle, pitch rate and stern planes are also shown as in figures 4 (b), (c) and (d).

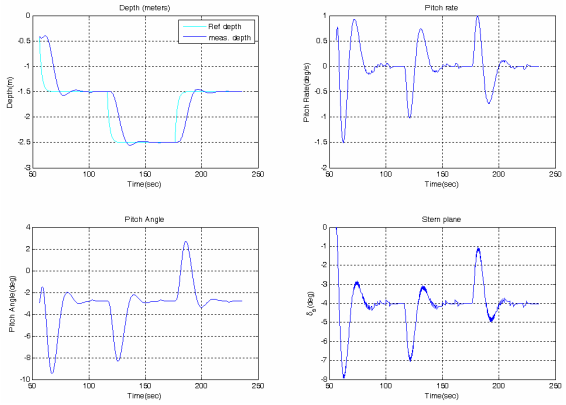

Figure 4 Simulation output: (a) depth (b) Pitch Angle (c) Pitch rate (d) Stern Planes

Time and frequency responses of the closed loop system demonstrate zero steady state error in response to step commands in depth (figure 5)

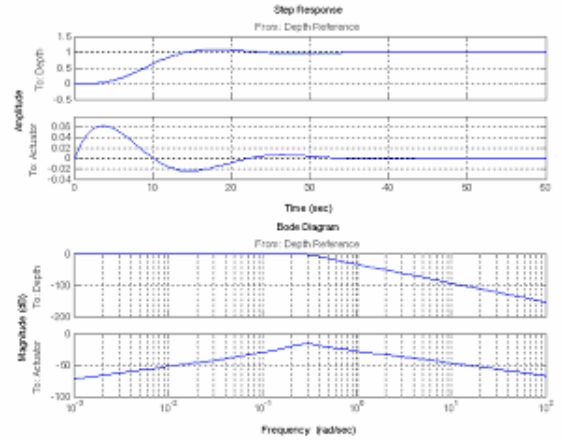

Figure 5 (a) Step response (b) Frequency response

3.2 Implementation and Field Results

The controller was based on the simulated condition described in section 3.1 and is implemented on a high performance embedded PC104. The controller loops in the software are set to run at 10 Hz.

Depth control of Maya was tested at Amthane Lake in Goa in early 2006 and the results are shown in figure 6. The comparison of time responses in depth for simulation and actual test match each other closely. The steady state pitch angle to maintain a depth in simulation is 1˚ less than the actual test data. A possible reason for this could be that the net positive buoyancy used in simulation could be slightly different from that realized in the field.

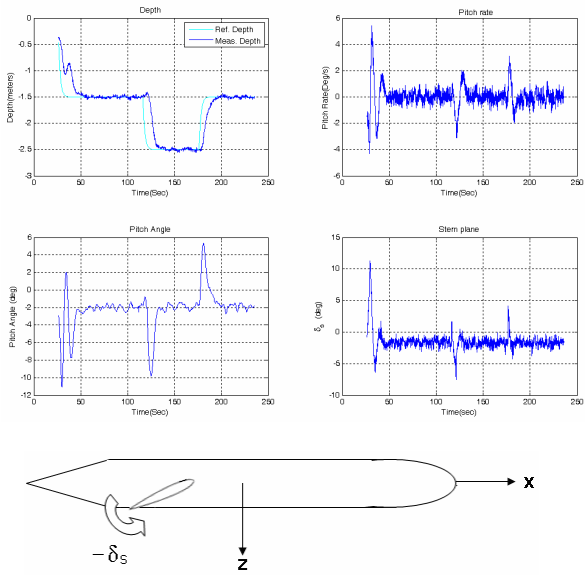

Figure 6 Field Test results: (a) depth (b) Pitch Angle (c) Pitch rate (d) Stern Panes (e) Sign convention for stern planes in Maya (the signs are opposite in Model and Actual data, what is plotted in fig 4(d) is negative of stern planes)

Encouraged by the close agreement between simulation and actual performance at Amthnem, Goa, Maya was then further tested at Idukki Lake in Kerala for a depth up to 21 meters in a stair case mission. The results of the dives are shown in figure 7.

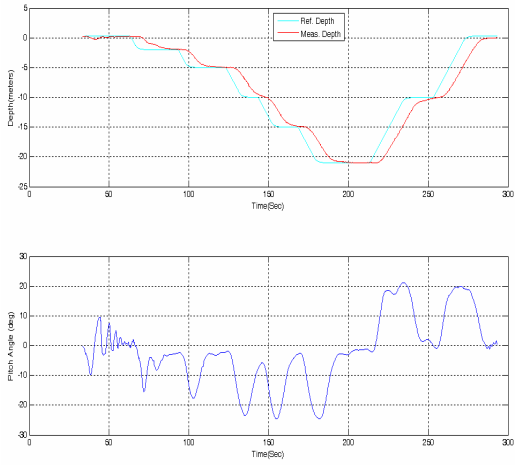

Figure 7 Stair case missions at Idukki:(a) Depth (b) Pitch Angle

The high pitch angles (20^0 to 25^0) during the staircase case change in depth are due to the low meta-centric height of ~7mm. The pitch excursions can be reduced by adjusting the rate limiter gain shown in figure 3.

4 CONTROL IN THE HORIZONTAL PLANE.

The control design technique used for heading control is similar to that used in the depth control system. As before, the horizontal plane model mentioned in (2) is used for the design of the heading

autopilot. However, in this case only two states [r, ψ] are accessible out of three [v, r, ψ] and the effect of sway is neglected.

4.1 Design and Simulation

The weight matrix used is given below

Weight matrixing: $Q = C^T C$

$C = [W_r \quad W_\psi \quad W_{\int\psi}] = [\ 0.8 \quad 1.5 \quad 0.7]$

$R = 0.1$

Gains $K = [\ -1.8338 \quad -2.7946 \quad -0.7\ ]$

Closed loop Eigen values are

Eigenvalue	Damping	Freq. (rad/s)
-3.76e-001 + 3.09e-001i	7.73e-001	4.87e-001
-3.76e-001 - 3.09e-001i	7.73e-001	4.87e-001
-1.22e+000	1.00e+000	1.22e+000

Bandwidth of the closed loop system is 0.412 rad/sec.

Figure 8(a) and 7(b) show the step and frequency responses of heading angle and actuator to command in heading, respectively.

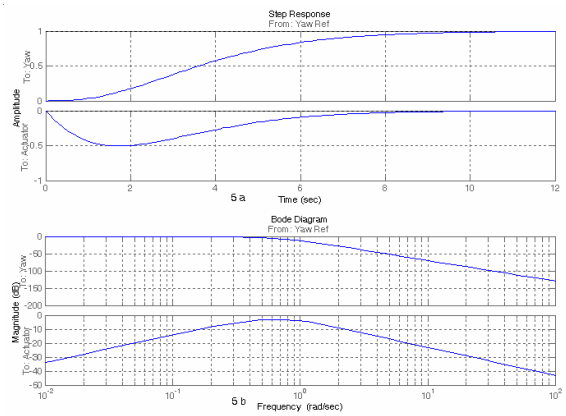

Figure 8 (a) Step response (b) Frequency response

The delta implementation of heading control system was simulated in Matlab™. The results of the simulation are shown in figure 8. A rate limiter at the input was not used in the case.

The resulting control law is

$$\delta = \int \left[K_3(\psi_d - \psi) - \frac{d}{dt}(K_1 r + K_2 \psi) \right] dt \qquad (7)$$

where ψ_d is desired heading, ψ is measured heading, and r is yaw rate.

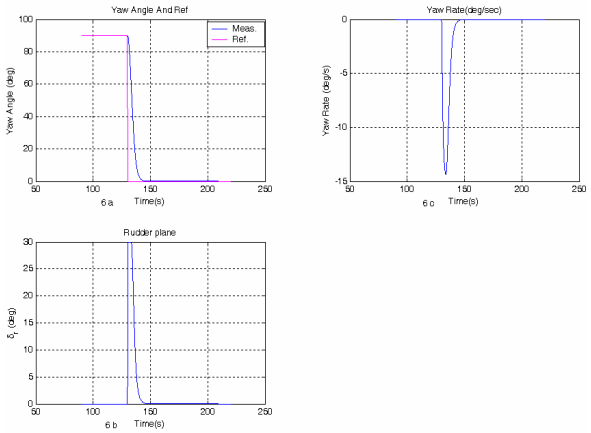

Figure 9 Simulation output (a) Heading angle (b) Rudder planes (c) Yaw rate

The field test data for heading control is shown in figure (10). The heading command of 0 degree was given while the vehicle was maintaining heading of 90 degree. The time responses in heading for simulation and actual test show acceptable agreement. Sign convention in model and in actual AUV are opposite for Rudder planes (figure 10e).

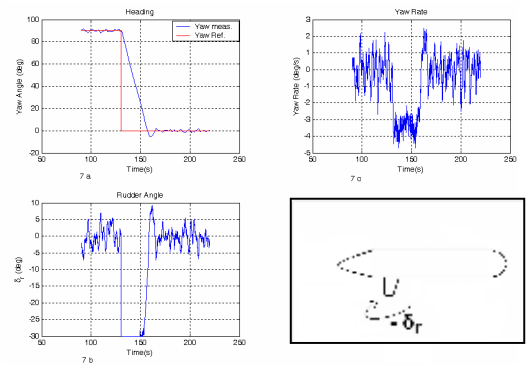

Figure 10 Field Test results (a) Heading angle (b) Rudder planes (c) Yaw rate (d) Sign convention in AUV for rudder plane

5. DEPTH-HEADING INTERACTION

As shown in fig 1, instead of having a rudder on top, a communication stub is mounted on the rudder port for convenience and testing. As a result of an asymmetry in control planes, an interaction between the heading and depth systems of Maya would be expected. Field test results shown in figure 11 confirm this expectation. It is observed that a change in heading during depth control causes a change in instantaneous depth. This is clearly captured in figures 11a and 11c which show the correspondence between reduction in depth and change in heading angle at the same time.

5.1 Qualitative Explanation of the Interaction

Balancing the forces in the vertical plane results in the condition

$$(B - W) = X \sin(\theta) + L_B(\alpha, Re) \quad (8)$$

where B is Buoyancy Force, W the weight of the vehicle, X the Surge force and L_B the body lift force which is a function of angle of attack (α) and Reynolds no(Re). A change in heading command disturbs the vertical plane balance resulting in the inequality

$$(B-W) > (X \sin(\theta) + L_B) \quad (9)$$

Heading change is brought about by a deflection in the rudder which generates the lift force L_r and a roll moment M_r about the C.G. of the vehicle and as a consequence a roll angle φ, see figure 12 (b). As there is only one rudder, there is practically no counter acting moment to prevent rolling of the vehicle (the metacentric height is small). As consequence of the uncompensated roll φ, the lift forces on the stern planes which are responsible for maintaining the depth are reduced by the factor cos(φ), with a consequent reduction in pitch angle (θ), pitching moment (M) and angle of attack (α). This leads to a reconfiguration of the balance in forces where, the net buoyancy force (B-W) overrides the downward ward Force X sin(θ) + L_B leading to inequality (9).

The stern and rudder plane angles are shown in figure 11b and the corresponding changes in roll and pitch angle are shown in figure 11d during the depth-heading interaction.

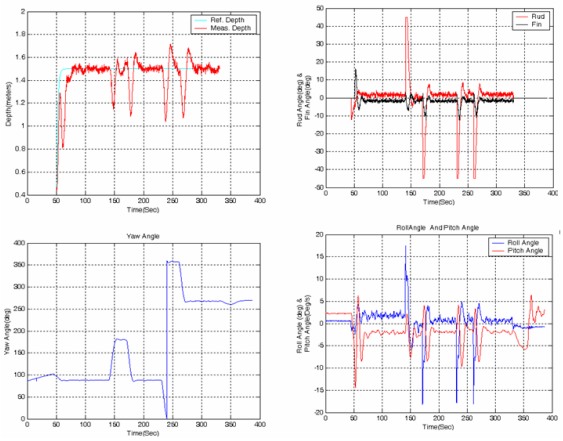

Figure 11 Field Test result for Heading and depth interaction (a) Depth (b) Control Planes (c) Yaw Angle (d) Pitch Angle and Roll Angle

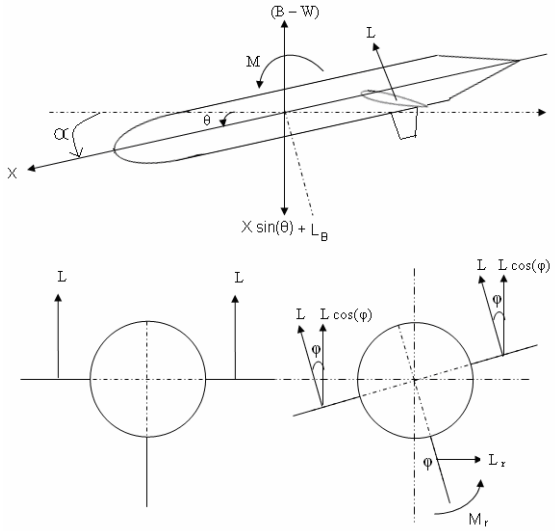

Figure 12. (a) Schematic of forces and moment for maintaining a depth. (b) Schematic of forces and moments for roll during turn.

6. CONCLUSIONS

Control systems for depth and heading control of a small AUV were designed and tested in field. The LQR methodology with delta implementation has proved useful in the development of the control systems for the MAYA AUV. The performance of controllers meets the requirement of performance and stability in both the vertical and horizontal planes. In addition, the delta implementation removes the bias from the stern planes obviating the need of a special sensor for precise measurement of control plane angles.

The use of three control planes and a low meta-centric height leads to an observed interaction between the depth and heading systems. A qualitative explanation of this effect has been presented in this paper.

Future work will address the problem of modeling the roll dynamics and designing an active roll compensation system. This is very important in shallow water surveys like bathymetry and bottom video/photography mosaicking. However, in oceanographic applications in which MAYA is being used, the roll effect can be tolerated.

ACKNOWLEDGEMENTS. We thank the DIT, New Delhi for the funding support extended to The National Institute of Oceanography, Marine Instrumentation Division, Goa on the development of the small AUV, MAYA. We also thank DST, New Delhi and GRICES, Portugal for exchange visit support under Indo-Portuguese Cooperation in S&T. A. Pascoal and L. Sebastião gratefully acknowledge the financial support of the AdI, Portugal (MAYASub project). The work of Ettore Barros was supported by the FAPESP Foundation in Brazil.

7. REFERENCES

Bjorn Jalving, “The NDRE-AUV Flight control system.”, *IEEE Journal of Ocean Engineering*, Vol. 19, No 4, October 1994.

E.A. de Barros, A. Pascoal, E de Sa, “AUV Dynamics: Modeling and parameter estimation using analytical and semi-empirical, and CFD methods”, *Proceeding of the CAMS IFAC Conference*, Ancona, Italy, 2004. [The data used is from a revised version of this paper which is to be published]

B. J Lurie, P.J. Enright, *Classical Feedback Control with Matlab,* Marcel Dekker Inc. New York, 2000.

Isaac Kaminer, A. Pascoal, Pramod Khargonekar and Edward E. Coleman, “A velocity algorithm for the implementation of gain-scheduled controllers*” Automatica*, Vol 31, No. 8, pp 1185 -1191, 1995.

SNAME(1950), “The Society of Naval Architects and Marine Engineers. Nomenclature for treating the motion of submerged body through a fluid.” *Technical Research Bulletin* No. 1-5